

Three-dimensional Vascular Imaging of Proliferative Diabetic Retinopathy by Doppler Optical Coherence Tomography



MASAHIRO MIURA, YOUNG-JOO HONG, YOSHIAKI YASUNO, DAISUKE MURAMATSU, TAKUYA IWASAKI, AND HIROSHI GOTO

- **PURPOSE:** To evaluate the 3-dimensional architecture of neovascularization in proliferative diabetic retinopathy using Doppler optical coherence tomography (OCT).
- **DESIGN:** Prospective, nonrandomized clinical trial.
- **METHODS:** Seventeen eyes of 14 patients with proliferative diabetic retinopathy were prospectively studied. Prototype Doppler OCT was used to evaluate the 3-dimensional vascular architecture at vitreoretinal adhesions.
- **RESULTS:** Proliferative membranes were detected in all eyes with proliferative diabetic retinopathy by standard OCT images. Doppler OCT images detected blood flow by neovascularization of the disc in 12 eyes and neovascularization elsewhere in 11 eyes. Doppler OCT images showed the 3-dimensional extent of new vessels at various stages of neovascularization, and the extent of new vessels could be clearly confirmed at vitreoretinal adhesions.
- **CONCLUSIONS:** Doppler OCT is useful for the detection and evaluation of the 3-dimensional vascular structure of neovascularization, and can assist in the noninvasive assessment of proliferative diabetic retinopathy. (Am J Ophthalmol 2015;159:528–538. © 2015 The Authors. Published by Elsevier Inc. All rights reserved. This is an open access article under the CC BY-NC-SA license (<http://creativecommons.org/licenses/by-nc-sa/3.0/>).)

PROLIFERATIVE DIABETIC RETINOPATHY (PDR) IS A major cause of visual loss in diabetic patients.^{1,2} Neovascularization of the disc and neovascularization elsewhere are characteristic findings of PDR, and cause vitreous hemorrhage and tractional retinal detachment.¹ Proper evaluation of neovascularization is therefore crucial for the diagnosis and treatment of this disorder.^{1,2} In current clinical practice, color fundus photography and biomicroscopy are basic techniques used to evaluate neovascularization; however, these techniques have

limited ability to detect the early stages of new vessel development.³ Fluorescein angiography is a powerful technique to detect the early stages of new vessels. However, clinical applications of fluorescein angiography have been limited because of the remote possibility of severe complications.⁴ Furthermore, limited axial resolution of fluorescein angiography has impeded the evaluation of the 3-dimensional structure of the new vessels.⁵

Optical coherence tomography (OCT) is a noninvasive method that can achieve micrometer-level axial resolution in cross-sectional images of the retina.⁶ OCT has provided important information about the 3-dimensional structure of the neovascular complex in PDR.^{3,7,8} However, standard OCT is only sensitive to backscattering light intensity, and cannot provide information about blood flow. Because of this limitation, standard OCT has a limited ability to evaluate neovascularization. Doppler OCT is a functional extension of OCT technology that is capable of Doppler shifts arising from blood flow.^{9,10} It can provide 3-dimensional vascular images with micrometer-level axial resolution in cross-sectional images of the retina.¹¹ The clinical utility of Doppler OCT in evaluating the 3-dimensional vascular architecture of choroidal new vessels has already been reported.^{11–13} It is therefore possible that Doppler OCT can facilitate a more comprehensive evaluation of retinal neovascularization in PDR. In this study, we present the clinical application of Doppler OCT for characterization of PDR, and describe the 3-dimensional vascular architecture at the site of neovascularization.

METHODS

THIS PROSPECTIVE, NONRANDOMIZED STUDY WAS performed according to the tenets of the Declaration of Helsinki, and was prospectively approved by the Institutional Review Boards of the University of Tsukuba and Tokyo Medical University. The nature of the current study and the implications of participating in this research were explained to all study candidates, after which a written informed consent was obtained from each participant before any study procedures or examinations were performed.



Supplemental Material available at [AJO.com](http://ajoo.com).

Accepted for publication Dec 1, 2014.

From the Department of Ophthalmology, Tokyo Medical University, Ibaraki Medical Center, Ibaraki, Japan (M.M., D.M., T.I.); Department of Ophthalmology, Tokyo Medical University, Tokyo, Japan (M.M., D.M., T.I., H.G.); and Computational Optics Group, University of Tsukuba, Ibaraki, Japan (Y.-J.H., Y.Y.).

Inquiries to Masahiro Miura, Department of Ophthalmology, Tokyo Medical University, Ibaraki Medical Center, 3-20-1 Chuo, Ami, Inashiki, Ibaraki 3000395, Japan; e-mail: m-miura@tokyo-med.ac.jp

As controls, we examined 8 eyes of 8 healthy Japanese volunteers (4 men and 4 women; age range, 27–53 years; mean age, 36.1 years). For PDR cases, we evaluated 17 eyes of 14 Japanese patients with PDR (Table; 10 men, 4 women; age range, 30–72 years; mean age, 51.5 years). Eyes with severe cataracts or other eye diseases that interfered with Doppler OCT image quality were excluded from this study. The clinical diagnosis of PDR was made by color fundus photography or fluorescein angiography. Four patients had type 1 diabetes and 10 patients had type 2 diabetes. The average hemoglobin A1C in all enrolled patients was 8.6% (range, 6.3%–13.9%). The left eye of Subject 3 was diagnosed as early-stage preproliferative diabetic retinopathy and was evaluated for comparison.

A detailed description of the prototype Doppler OCT system, built by the Computational Optic Group at the University of Tsukuba, has been previously reported.^{13,14} This Doppler OCT was based on a swept-source technology, and operated at an axial scan speed of 100 000 A-scans/s, using a swept-source laser at a central wavelength of 1060 nm. The axial resolution for the tissue in this study was 6.4 μm. In a single scan, the system simultaneously provided both an intensity-based standard OCT image and a Doppler OCT image. The Doppler signal was calculated from 2 A-lines in 2 successive B-scans. Doppler signals were displayed in the form of the squared energy of the Doppler phase shift. Raster scanning protocol with 256 A-lines × 2048 B-scans covering a 6.0 × 6.0-mm region on the retina was used for volumetric scans. In 1 eye (Subject 4), raster scanning protocol with 256 A-lines × 2048 B-scans covering a 3.0 × 3.0-mm region on the retina was used to image intraretinal microvascular abnormalities (IRMA). To obtain a clear image of IRMA, the 3-dimensional Doppler OCT volume was automatically segmented to the retina and choroid, and the en face projection Doppler OCT image of the retina was used to localize the IRMA. The acquisition speed of each measurement was 6.6 s/volume.

RESULTS

• **NORMAL EYES:** Figure 1 shows Doppler OCT images of a representative 27-year-old healthy subject. The standard OCT image was similar to commercial high-resolution OCT. An en face projection image by standard OCT enabled precise registration of OCT data using color fundus photography. Doppler OCT B-scan images showed the cross-sectional distribution of blood flow in the retina. Composite color Doppler OCT images, in which the Doppler OCT signal was overlaid on the standard OCT with red color, were created from standard OCT and Doppler OCT images to specify the location of blood flow in the standard OCT image. An en face projection image by Doppler OCT clearly showed the chorioretinal vascular architecture.

TABLE. Proliferative Diabetic Retinopathy by Doppler Optical Coherence Tomography: Summary of Subjects

Subject	Age (y)	Sex	HBA1c (%)	Type of Diabetes	Eye	Neovascular Complex	Figure
1	61	M	9.7	2	OD	NVD	
					OS	NVD, NVE	2
2	45	F	9.9	1	OD	NVD, NVE	3,6
3	48	M	6.3	1	OD	NVE	5
4	55	M	6.5	2	OD	NVD, NVE	7
5	57	M	10.4	2	OS	NVD	
6	50	F	6.6	2	OD	NVE	
7	51	F	10.3	2	OD	NVD, NVE	
					OS	NVD, NVE	
8	39	M	10.3	1	OS	NVD	
9	66	M	8	2	OD	NVD	
					OS	NVD, NVE	
10	70	M	9.1	2	OS	NVD	
11	72	F	9	2	OD	NVE	
12	30	M	13.9	1	OS	NVE	
13	65	M	6.5	2	OD	NVE	
14	39	M	7.2	2	OS	NVD	

NVD = neovascularization of the disc; NVE = neovascularization elsewhere.

• **EARLY NEOVASCULARIZATION OF THE DISC:** Early neovascularization of the disc involves the neovascular complex within the margin of the optic disc (Figure 2). In 4 eyes, standard OCT and fluorescein angiography confirmed the presence of early neovascularization of the disc. Standard OCT shows a hyperreflective mass at the disc, accompanied by some loop formations. Doppler OCT composite images show the presence of neovascularization throughout the hyperreflective mass. In the early stage of neovascularization of the disc, the presence of neovascularization is often not detected using color fundus photography or biomicroscopy. In contrast, Doppler OCT imaging detected a neovascular complex with the presence of new vessels in the proliferative tissue.

• **ADVANCED NEOVASCULARIZATION OF THE DISC:** Ten eyes had advanced neovascularization of the disc. In the advanced stage, neovascular complexes extended beyond the margin of the optic disc and formed vitreoretinal traction (Figure 3). Using standard OCT images, hyperreflective masses became enlarged and covered the optic disc with multiple loop formations, while Doppler OCT showed the presence of new vessels in the hyperreflective neovascular complex.

In the right eye of Subject 2, Doppler OCT composite images showed an increase of new vessels. Using fluorescein angiography images, detailed evaluation of new vessels was impeded by active fluorescein leakages. In contrast, the fine structure of new vessels was clearly detected in Doppler

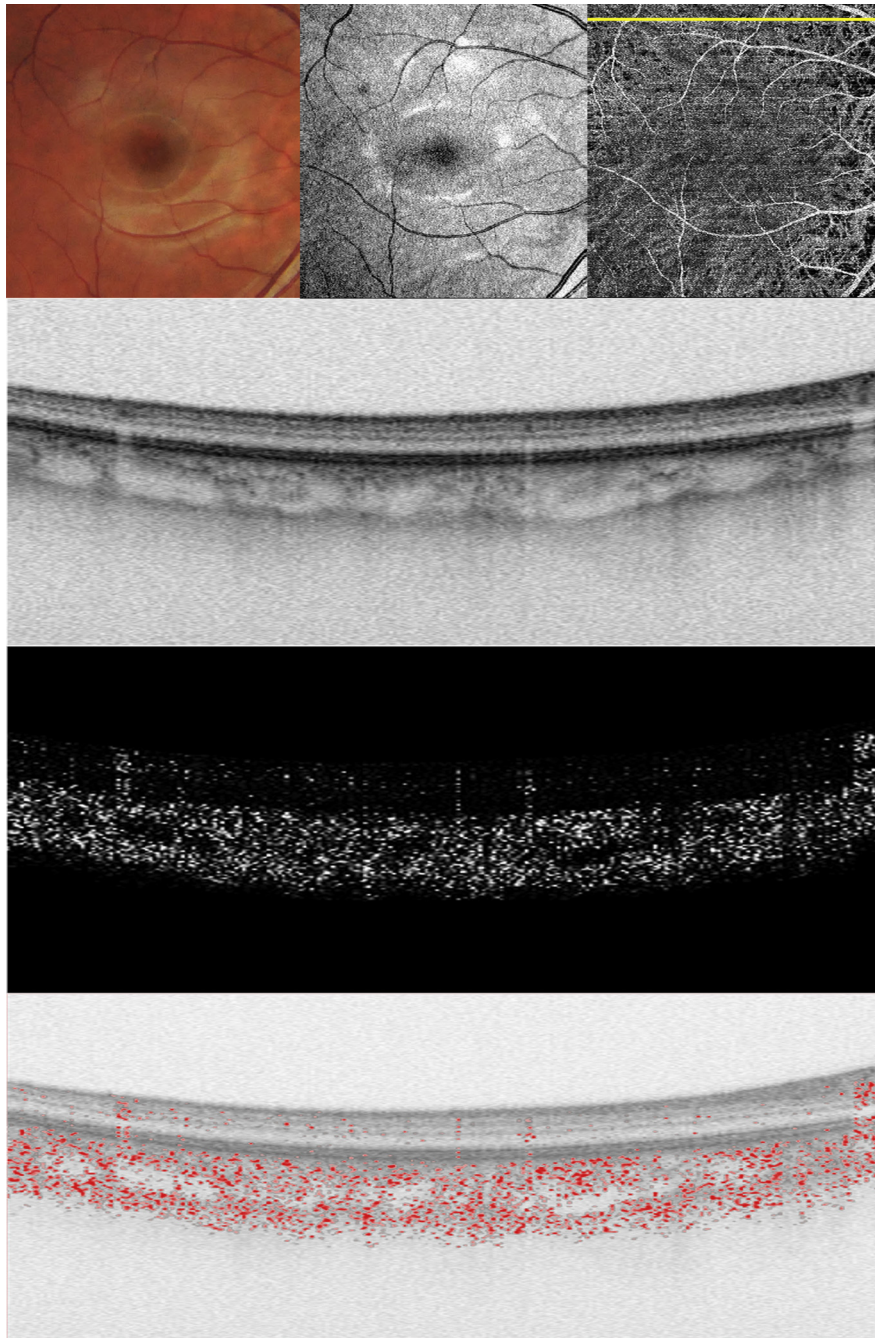


FIGURE 1. Doppler optical coherence tomography (OCT) images of a healthy subject. An en face projection image by standard OCT (Top row, middle) enabled precise registration of OCT data with a color fundus photograph (Top row, left). An en face projection image using the Doppler OCT image (Top row, right) shows a retinal vascular pattern. The yellow line specifies the scanning line of the B-scan OCT image. A composite OCT image (Bottom row) was created from a standard OCT image (Second row) and a Doppler OCT image (Third row).

OCT imaging because of its impervious feature to fluorescein leakage (Figure 3). An enlargement of the area of new vessels could be easily identified with a Doppler OCT en face image. In this eye, the neovascular complex was attached to a remnant of the Cloquet canal. Standard OCT could not confirm whether the neovascularization

extended into this vitreoretinal traction, while Doppler OCT readily confirmed the absence of blood flow at a remnant of the Cloquet canal.

Figure 4 shows the left eye of Subject 2. Fluorescein angiography images show an early stage of preproliferative diabetic retinopathy without neovascularization of the disc.

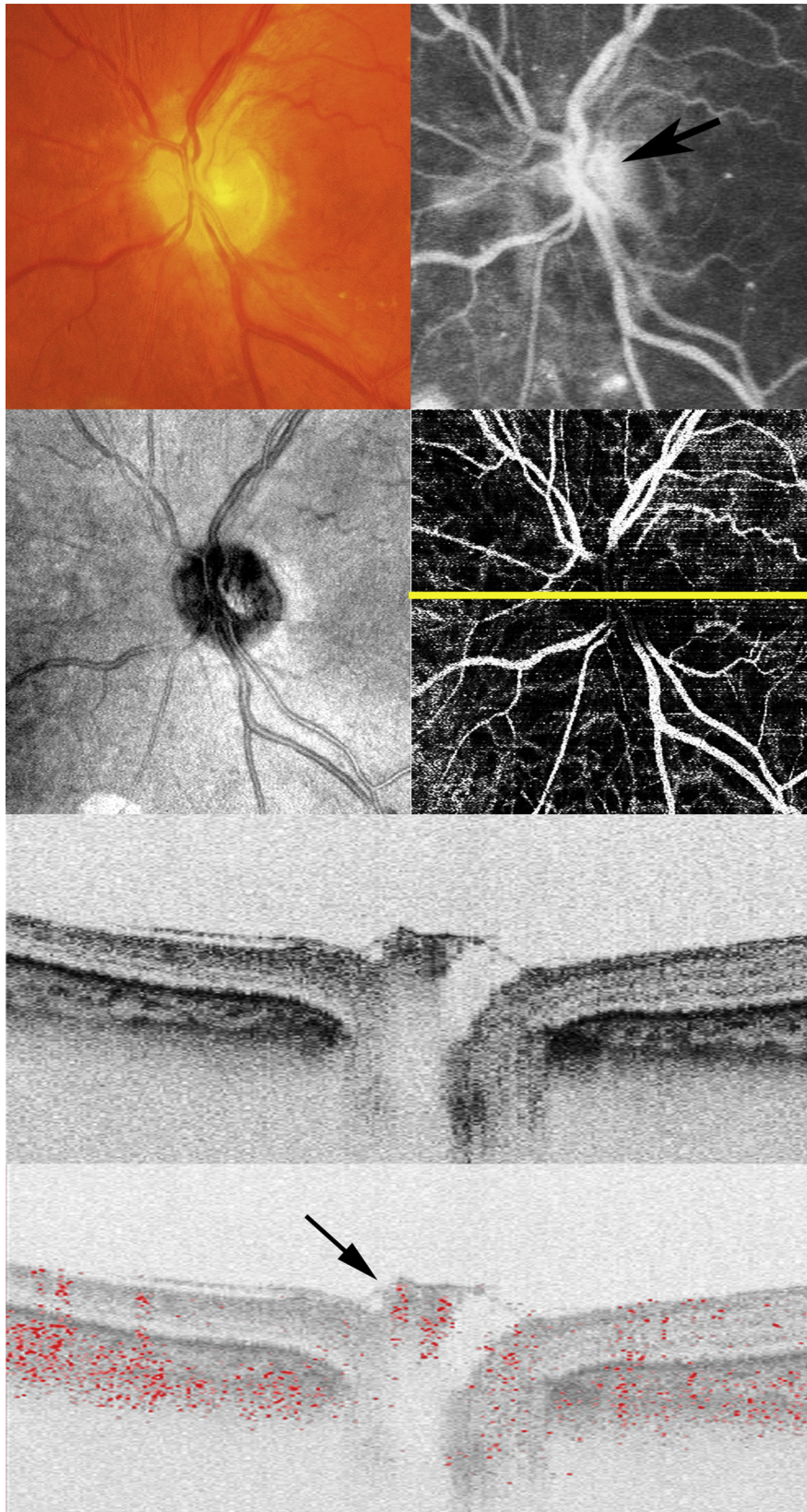


FIGURE 2. Doppler optical coherence tomography (OCT) images from the left eye of Subject 1 with early neovascularization of the disc in proliferative diabetic retinopathy. Fluorescein angiography (Top row, right) shows fluorescein leakage (black arrow) from a new vessel on the disc. An en face projection image using standard OCT (Second row, left) enabled precise registration of OCT data with color fundus photography (Top row, left). The yellow line in the en face projection image using Doppler OCT (Second row,

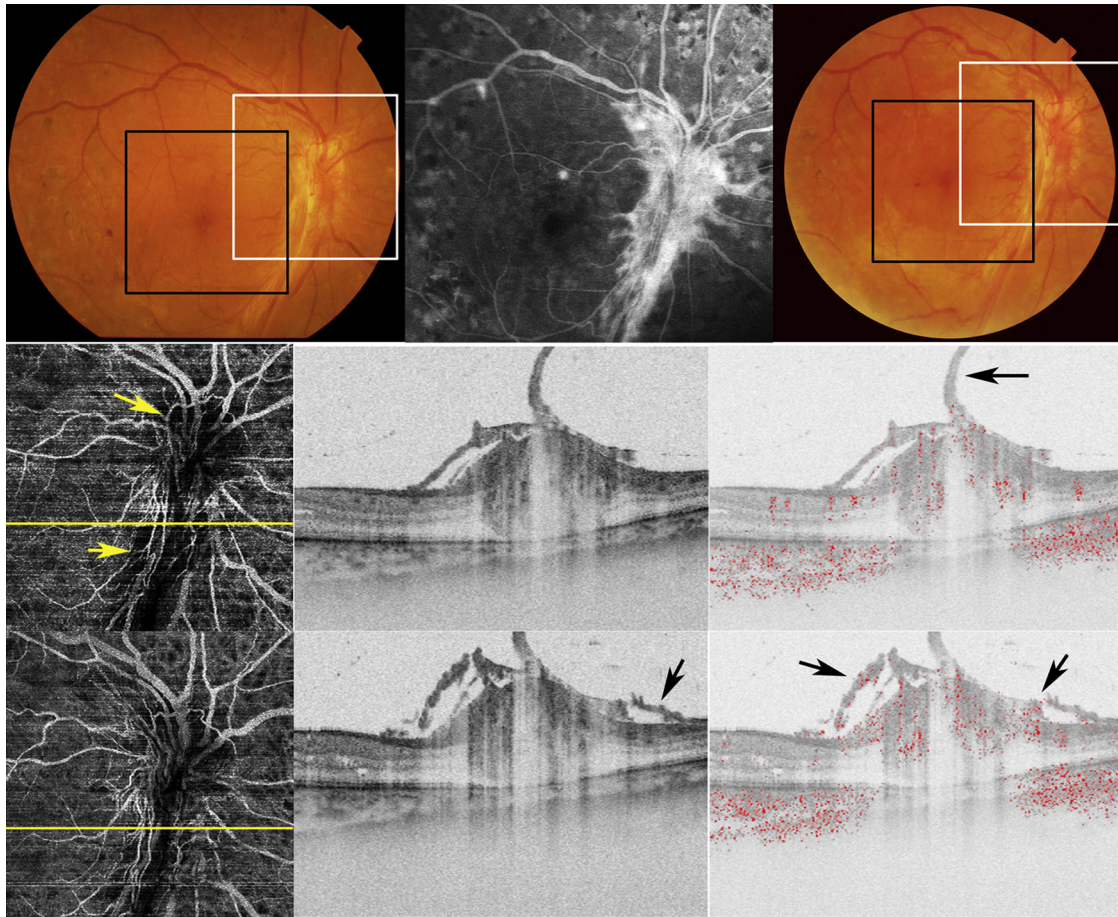


FIGURE 3. Doppler optical coherence tomography (OCT) images of the right eye of Subject 2 with advanced neovascularization of the disc in proliferative diabetic retinopathy. The white lines in the color fundus photographs at first measurement (Top row, left) and at 3 months after the first measurement (Top row, right) indicate the scanning areas of the Doppler OCT images on the disc (Second row and Third row), and the black lines indicate the scanning areas of the Doppler OCT images on the macula (Figure 6, Second row and Third row). Fluorescein angiography at first measurement (Top row, middle) shows fluorescein leakage from the neovascularization. (Second row) The Doppler OCT image of the disc at first measurement. An en face projection image by Doppler OCT (left) shows new vessels on the proliferative tissue (yellow arrows). The yellow line specifies the scanning line of the B-scan OCT image. The standard OCT image (middle) shows proliferative tissue on the disc with multiple loop formations. Proliferative tissue was attached to a remnant of the Cloquet canal. The Doppler OCT composite image (right) shows the absence of new vessels at a remnant of the Cloquet canal (black arrow). (Third row) A Doppler OCT image of the disc at 3 months after first measurement. Enlargement of new vessels was confirmed by an en face projection image using Doppler OCT (left). The yellow line specifies the scanning line of the B-scan OCT image. A standard OCT image (middle) shows an increase of proliferative tissue (black arrow). A Doppler OCT composite image (right) shows enlargement of new vessels in the proliferative tissue (black arrow).

The standard OCT image shows adhesion of a remnant of the Cloquet canal on the optic disc. An absence of new vessels in this vitreoretinal adhesion was confirmed by a Doppler OCT composite image, illustrating the usefulness of Doppler OCT to confirm the existence of new vessels at vitreoretinal adhesions.

Because of traction to the neovascular complex, tractional retinal detachment developed in 3 eyes. The detached retina lost its architecture, and standard OCT showed tractional retinal detachment and deformed loop formation in the neovascular complex. A Doppler OCT composite image showed the presence of new vessels in

right) specifies the scanning line of the B-scan OCT image (Third row and Bottom row). A standard OCT image (Third row) shows a hyperreflective mass with loop formation on the disc. A Doppler OCT composite image (Bottom row) shows the presence of new vessels throughout the neovascular complex (black arrow).

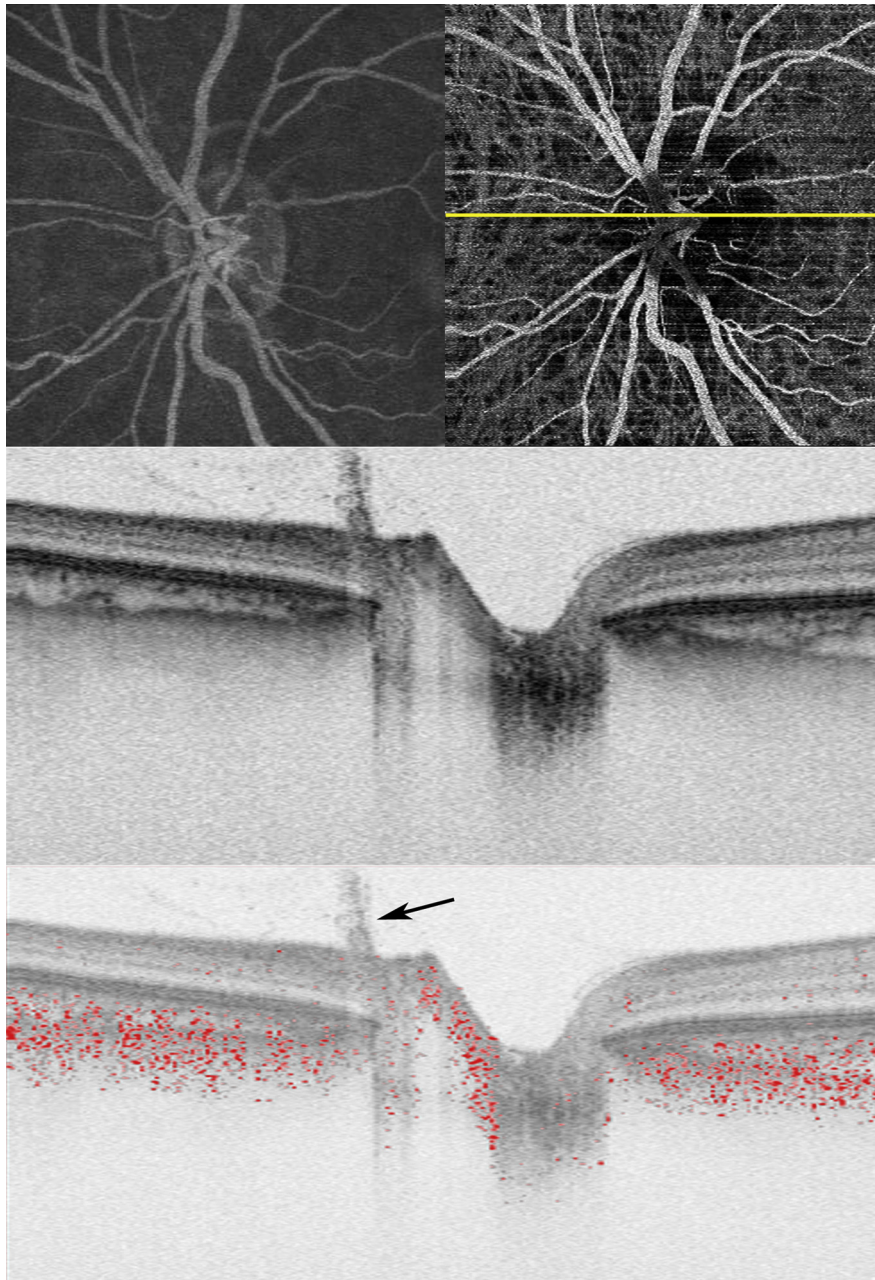


FIGURE 4. Doppler optical coherence tomography (OCT) imaging of the left eye of Subject 2 with nonproliferative diabetic retinopathy. Fluorescein angiography (Top row, left) shows the absence of new vessels in the disc. The yellow line in the en face projection image using Doppler OCT (Top row, right) specifies the scanning line of the Doppler OCT B-scan image. A standard OCT image (Second row) shows an adhesion to a remnant of the Cloquet canal. The absence of blood flow in this adhesion was confirmed by the Doppler OCT composite image (Third row, black arrow).

the neovascular complex. At the vitreoretinal traction site, new vessels were pulled toward the vitreous, and the amount of displacement could be easily identified by Doppler OCT images (Supplemental Figure 1, available at AJO.com).

- **INNER RETINAL NEOVASCULARIZATION:** One eye showed neovascularization in the inner retina (Figure 5).

The presence of neovascularization was confirmed by fluorescein angiography. Standard OCT showed a focal hyperreflective mass, located in the inner retinal layers. Focal hyperreflective lesions extended through the inner plexiform layer, ganglion cell layer, and nerve fiber layer. Doppler OCT imaging confirmed the presence of blood flow at neovascularization in this hyperreflective mass.

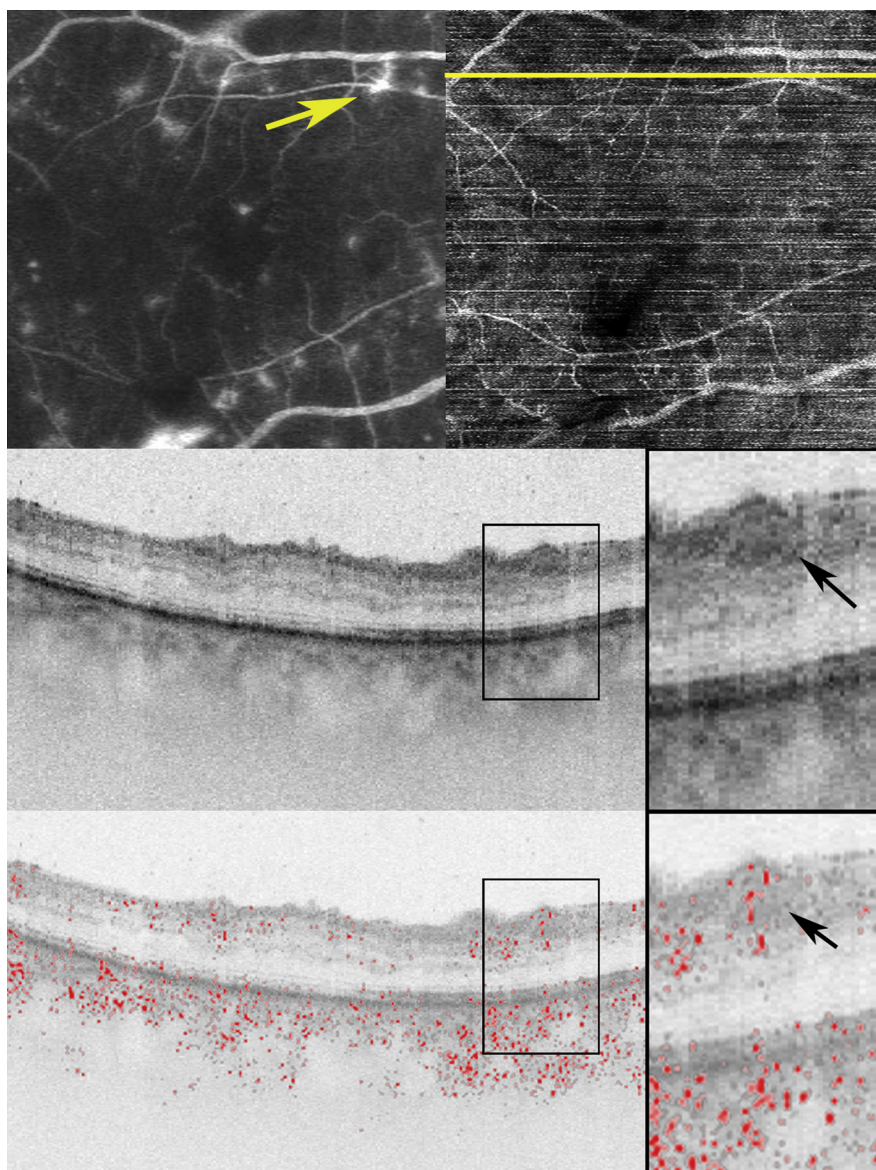


FIGURE 5. Doppler optical coherence tomography (OCT) imaging of the left eye of Subject 3 with inner retinal neovascularization in proliferative diabetic retinopathy. Fluorescein angiography (Top row, left) shows fluorescein leakage from the neovascularization (yellow arrow). The yellow line in the en face projection image using Doppler OCT (Top row, right) specifies the scanning line of the Doppler OCT B-scan image. The black line in the standard OCT image (Second row, left) is an area of high magnification at the inner retinal neovascularization site (Second row, right). A standard OCT image shows the presence of hyperreflective lesions in the inner retinal layer at the neovascularization site (black arrow). The black line in the Doppler OCT composite image (Third row, left) is an area of high magnification at the inner retinal neovascularization (Third row, right). The Doppler OCT composite image shows the presence of blood flow in the inner retinal neovascularization site (black arrow).

• **ADVANCED NEOVASCULARIZATION ELSEWHERE:** Nine eyes had advanced neovascularization elsewhere. In advanced neovascularization elsewhere, hyperreflective lesions extended through the internal limiting membrane and were composed of mushroom-like structures in the retina (Figure 6). Doppler OCT confirmed the presence of blood flow at neovascularization sites. After growth, the mushroom-like structures contained hyporefective spaces (Figure 6). Doppler OCT showed loop formation

of new vessels surrounding the hyporefective spaces (Figure 6). Consecutively, the hyperreflective neovascular complexes formed vitreoretinal adhesion, and the neovascular complex was pulled toward the vitreous body. Doppler OCT confirmed that new vessels were near the apex of the hyperreflective mass. The presence of these new vessels suggested the risk of vitreous hemorrhage following contraction of the vitreous body. In the case of multiple neovascularizations elsewhere, new vessels grew

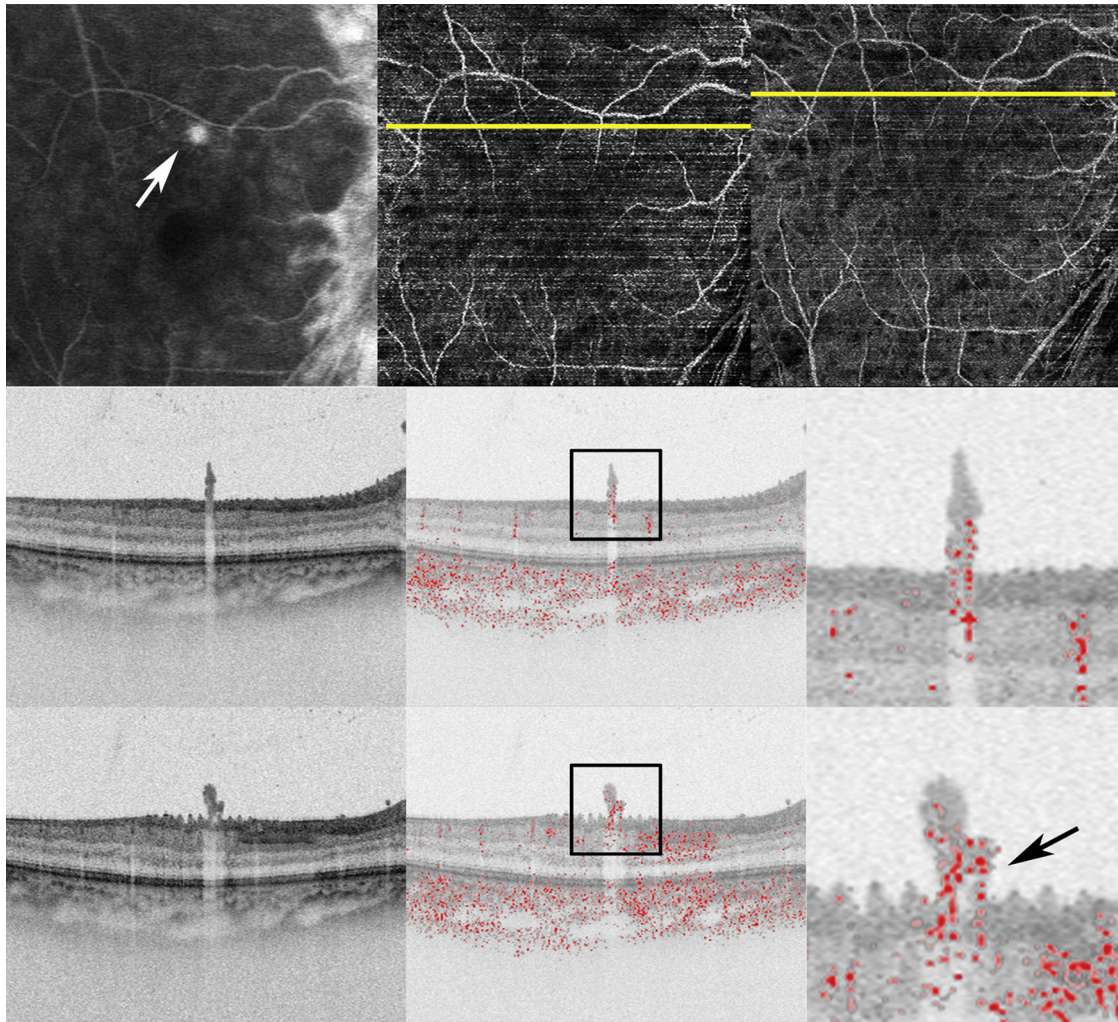


FIGURE 6. Doppler optical coherence tomography (OCT) imaging of the macula of the right eye of Subject 2 with advanced neovascularization elsewhere in proliferative diabetic retinopathy. Fluorescein angiography (Top row, left) shows fluorescein leakage from the neovascularization site (white arrow). Yellow lines in the en face projection image using Doppler OCT at first measurement (Top row, middle) and at 3 months after the first measurement (Top row, right) indicate scanning lines of Doppler OCT imaging at the first measurement (Second row, left) and at 3 months after the first measurement (Third row), respectively. A standard OCT image at first measurement (Second row, left) shows proliferative tissue in the retina. The black line in the Doppler OCT composite image at first measurement (Second row, middle) indicates the area of high magnification (Second row, right). The Doppler OCT composite image shows new vessels in the proliferative tissue. Standard OCT image at 3 months after the first measurement (Third row, left) shows proliferative tissue with a hyporeflective space. The black line in the Doppler OCT composite image at 3 months after the first measurement (Third row, middle) specifies the area of high magnification (Third row, right). The Doppler OCT composite image shows a loop formation by new vessels surrounding the hyporeflective space (black arrow).

as pillars between the retina and the proliferative membrane (Supplemental Figure 2, available at AJO.com).

• **INTRARETINAL MICROVASCULAR ABNORMALITIES:** One eye showed IRMA in fluorescein angiography images. IRMA was confirmed by the presence of dilated, tortuous, vascular segments without early fluorescein leakage (Figure 7). A retinal en face projection Doppler OCT image of the retina showed a clear image of the IRMA, and Doppler OCT imaging confirmed the presence of blood flow by IRMA in the inner plexiform layer. In contrast to

inner retinal neovascularization, the hyperreflective lesion was not confirmed in the area of IRMA in the standard OCT image.

DISCUSSION

STANDARD OCT HAS BECOME AN ESSENTIAL MODALITY IN the management of diabetic retinopathy.¹⁵ It allows the clinician to detect and monitor neovascularization in various stages of PDR.^{3,7,8,16} However, standard OCT

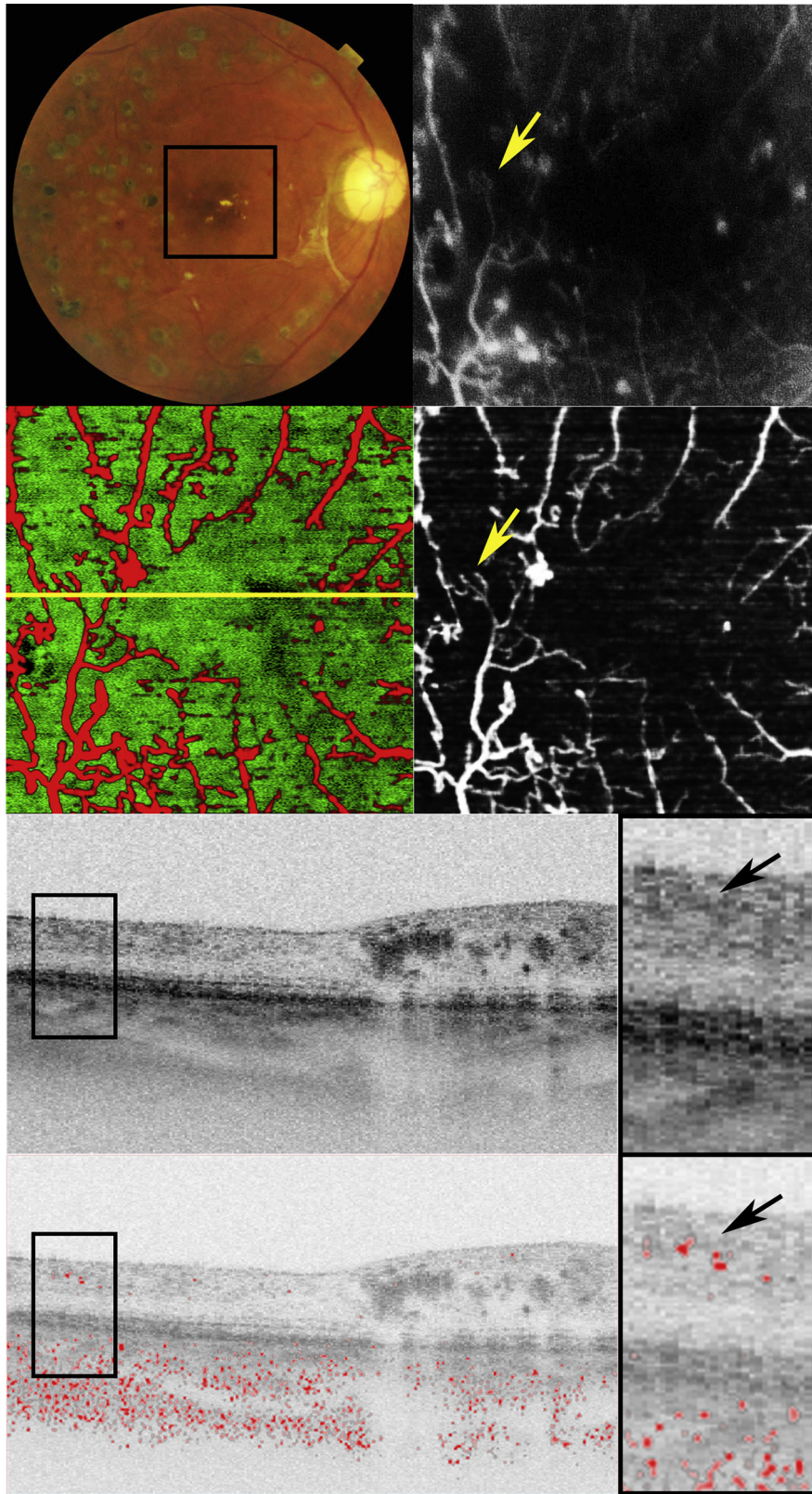


FIGURE 7. Doppler optical coherence tomography (OCT) image of the right eye of Subject 4 with intraretinal microvascular abnormalities (IRMA) in proliferative diabetic retinopathy. Color fundus photography (Top row, left) shows proliferative tissue in the disc. The black line indicates the area of fluorescein angiography and Doppler OCT imaging. A fluorescein angiography image (Top row, right) shows IRMA without fluorescein leakage (yellow arrow). Composite en face projection of the Doppler OCT image (Second row, left) shows clear images of the retinal vessels (red color) after separation from the choroidal Doppler OCT image (green color).

cannot discriminate vascular lesions from the surrounding tissues; hence, standard OCT can only provide limited information about the location of the neovascularization. Recently, a functional extension of OCT technology for 3-dimensional vascular imaging was developed. This technique was first reported using Doppler OCT and was named optical coherence angiography.¹⁷ Following this development, several phase-based^{11–13,17–20} and intensity-based^{21–23} 3-dimensional vascular imaging techniques were reported, and were collectively called OCT angiography. The clinical utilities of OCT angiography have been reported for polypoidal choroidal vasculopathy,^{11–13} choroidal neovascularization,^{13,22,20} and preproliferative diabetic retinopathy.²⁰ Unlike standard OCT, OCT angiography can directly evaluate vascular architecture, including a comprehensive evaluation of vascular lesions.

In the present study, we used Doppler OCT to investigate the vascular architecture in PDR. A combination of standard OCT images and Doppler images provided comprehensive information about the development of neovascularization. In cases of neovascularization of the disc, neovascularization was enlarged laterally toward the outside of the optic discs, and Doppler OCT confirmed an increase of new vessels in proliferative tissue. In the case of inner retinal neovascularization, Doppler OCT imaging confirmed the presence of new vessels in the inner retinal layer. After breaking through the internal limiting membrane, new vessels in neovascularization formed loop formations and were pulled toward the vitreous body. The 3-dimensional distribution of neovascularization in PDR could provide important information to be used in the surgical treatment of PDR.²⁴ If new vessels are attached to the posterior hyaloid membrane, a high risk of vitreous hemorrhage must be considered. Surgical intervention of proliferative tissue with new vessels has a higher risk of bleeding during surgery. In contrast, vitreoretinal traction without new vessels could be easily handled during vitrectomy. This information should therefore be important for the surgical planning of PDR. Furthermore, Doppler OCT imaging might be applicable to evaluate the therapeutic effect for neovascularization in PDR, such as laser photocoagulation or anti-vascular endothelial growth factor therapy. This study did not evaluate the capillary nonperfusion area, but capillary nonperfusion is an important finding for treatment strategies. Further studies are required to evaluate the clinical utility of Doppler OCT for the treatment of PDR.

In a previous study using standard OCT, IRMA were observed as hyperreflective lesions in the inner retinal

layers, and focal protrusions through the inner limiting membrane at IRMA were reported.⁸ In the present study, hyperreflective lesions could not be confirmed in the area of blood flow by IRMA. The presence of hyperreflective lesions in the inner retinal layers was a characteristic finding in inner retinal neovascularization. In a clinicopathologic report, IRMA were consistent with vascular pathology typical for intraretinal microangiopathy, but also included new vessels in some cases.²⁵ Variations of vascular architecture at IRMA might be a possible reason for the differences of the present study when compared with a previous report.⁸ Based on these results, in future studies, a larger number of patients is required to fully evaluate the fine vascular architecture at the IRMA.

There are several limitations to the present study using Doppler OCT. Fluorescein leakage in fluorescein angiography is an important indication of neovascularization, but Doppler OCT cannot detect fluorescein leakage; hence, fluorescein angiography imaging is required for the diagnostic confirmation of inner retinal neovascularization. In the present study, 6.6 seconds were required for a single measurement, despite using high-speed 100 kHz OCT. This relatively long measurement time caused motion artifacts in vascular imaging. A motion correction algorithm using orthogonal scan patterns might be a possible solution.²⁶ Another possible solution would be using ultra-high-speed OCT. Clinical applications of multi-MHz OCT have already been reported,²⁷ so the influence of motion artifacts could be compensated by shortening of measurement times.

In conclusion, this study demonstrated the clinical utility of Doppler OCT to evaluate neovascular complexes in PDR. Doppler OCT could detect only some retinal vascular changes; hence, fluorescein angiography is still required to evaluate diabetic retinopathy. Fluorescein angiography is an important diagnostic modality to detect neovascularization. However, fluorescein angiography cannot provide 3-dimensional information because of its poor axial resolution. In addition, evaluation of the fine microvascular structure at neovascularization was significantly impeded by fluorescein leakage from new vessels. Doppler OCT imaging was impervious to leakage from new vessels and provided comprehensive 3-dimensional vascular information of neovascularization. Clinical applications of fluorescein angiography have been limited because of patient discomfort and the relatively long measurement times. In contrast, Doppler OCT imaging is noninvasive and has a short measurement time, and may therefore provide a noninvasive alternative to fluorescein angiography in assessing PDR.

The yellow line specifies the scanning line of the Doppler OCT B-scan image (Third row and Bottom row). An en face projection Doppler OCT image of the retina (Second row, right) shows a clear image of the IRMA (yellow arrow). The black line in the standard OCT image (Third row, left) is an area of high magnification at the IRMA (Third row, right). Using a standard OCT image, no specific lesion was detected in the area with IRMA (black arrow). The black line in the Doppler OCT composite image (Third row, left) is an area of high magnification at the IRMA (Third row, right). The Doppler OCT composite image shows the presence of blood flow at the IRMA (black arrow).

ALL AUTHORS HAVE COMPLETED AND SUBMITTED THE ICMJE FORM FOR DISCLOSURE OF POTENTIAL CONFLICTS OF INTEREST. Financial Disclosures: Masahiro Miura received a lecture fee from Novartis Pharma AG, Basel, Switzerland. Computational Optics Group, University of Tsukuba received funding support from Tomey (Nagoya, Japan), Topcon (Tokyo, Japan), and Nidek (Gamagori, Japan). This study is supported by a Grant-in-Aid for Scientific Research (KAKENHI 24592682) from the Japan Society for the Promotion of Science, Tokyo, Japan. Contributions of authors: conception and design (M.M., Y.-J.H., Y.Y., D.M.); analysis and interpretation (M.M., Y.-J.H., Y.Y., D.M., T.I., H.G.); writing the article (M.M.); critical revision of the article (M.M., Y.-J.H., Y.Y., D.M., T.I., H.G.); final approval of the article (M.M., Y.-J.H., Y.Y., D.M., T.I., H.G.); data collection (M.M., D.M.); provision of materials, patients, or resources (M.M., Y.-J.H., Y.Y., D.M., T.I.); statistical expertise (M.M.); obtaining funding (M.M., Y.Y., T.I., H.G.); literature search (M.M., Y.-J.H.); administrative technical or logistic support (M.M., Y.Y., T.I., H.G.).

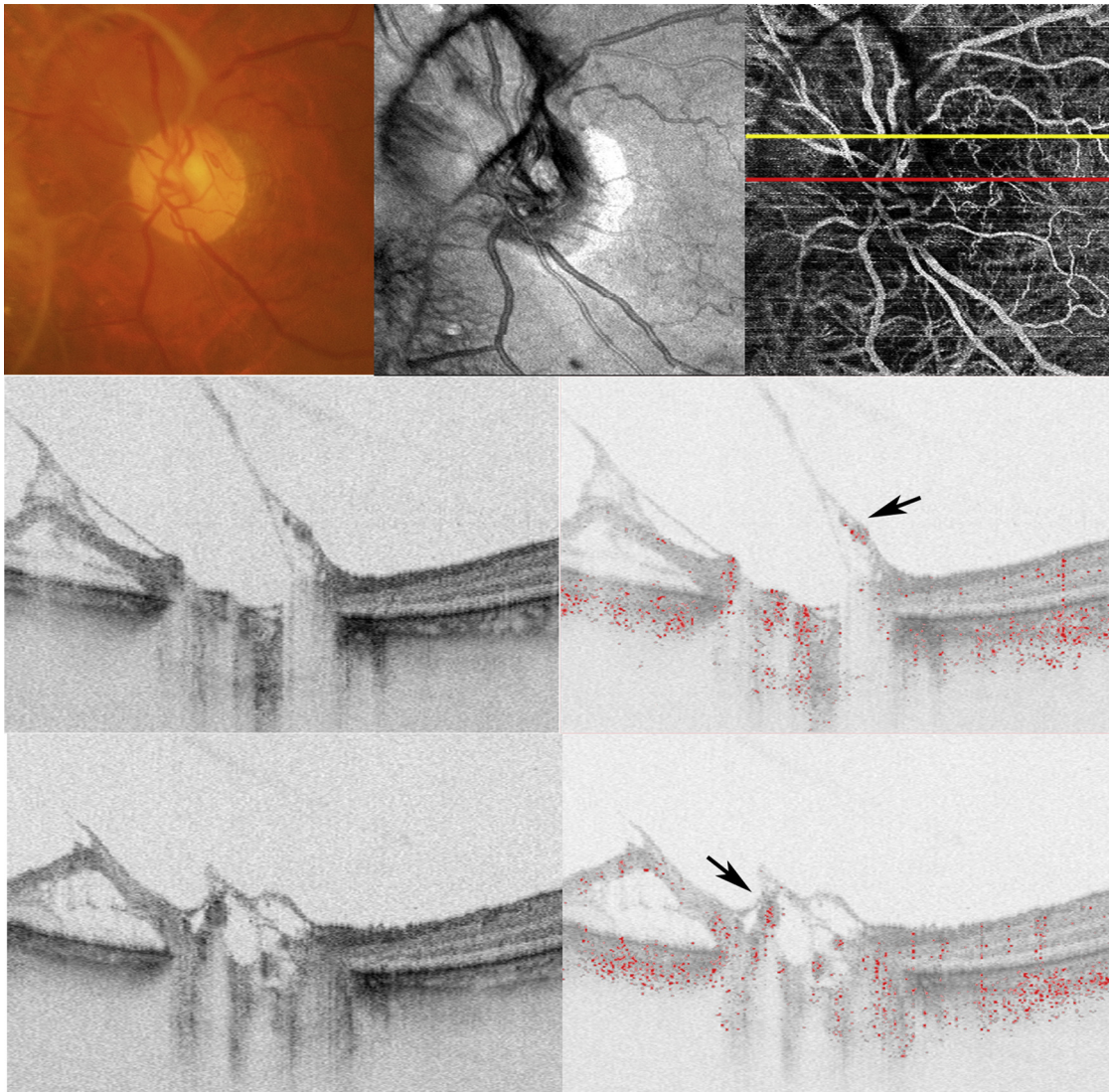
REFERENCES

1. Davis MD. Diabetic retinopathy. A clinical overview. *Diabetes Care* 1992;15(12):1844–1874.
2. Frank RN. Diabetic retinopathy. *N Engl J Med* 2004;350(1):48–58.
3. Muqit MM, Stanga PE. Fourier-domain optical coherence tomography evaluation of retinal and optic nerve head neovascularisation in proliferative diabetic retinopathy. *Br J Ophthalmol* 2014;98(1):65–72.
4. Yannuzzi LA, Rohrer KT, Tindel LJ, et al. Fluorescein angiography complication survey. *Ophthalmology* 1986;93(5):611–617.
5. Bartsch DU, Freeman WR. Axial intensity distribution analysis of the human retina with a confocal scanning laser tomograph. *Exp Eye Res* 1994;58(2):161–173.
6. Huang D, Swanson E, Lin C, et al. Optical coherence tomography. *Science* 1991;254(5035):1178–1181.
7. Iwasaki T, Miura M, Matsushima C, Yamanari M, Makita S, Yasuno Y. Three-dimensional optical coherence tomography of proliferative diabetic retinopathy. *Br J Ophthalmol* 2008;92(5):713.
8. Cho H, Alwassia AA, Regiatieri CV, et al. Retinal neovascularization secondary to proliferative diabetic retinopathy characterized by spectral domain optical coherence tomography. *Retina* 2013;33(3):542–547.
9. Izatt JA, Kulkarni MD, Yazdanfar S, Barton JK, Welch AJ. In vivo bidirectional color Doppler flow imaging of picoliter blood volumes using optical coherence tomography. *Opt Lett* 1997;22(18):1439–1441.
10. Leitgeb R, Schmetterer L, Drexler W, Fercher A, Zawadzki R, Bajraszewski T. Real-time assessment of retinal blood flow with ultrafast acquisition by color Doppler Fourier domain optical coherence tomography. *Opt Express* 2003;11(8):3116–3121.
11. Miura M, Makita S, Iwasaki T, Yasuno Y. Three-dimensional visualization of ocular vascular pathology by optical coherence angiography in vivo. *Invest Ophthalmol Vis Sci* 2011;52(5):2689–2695.
12. Makita S, Jaillon F, Yamanari M, Miura M, Yasuno Y. Comprehensive in vivo micro-vascular imaging of the human eye by dual-beam-scan Doppler optical coherence angiography. *Opt Express* 2011;19(2):1271–1283.
13. Hong YJ, Miura M, Makita S, et al. Noninvasive investigation of deep vascular pathologies of exudative macular diseases by high-penetration optical coherence angiography. *Invest Ophthalmol Vis Sci* 2013;54(5):3621–3631.
14. Hong YJ, Makita S, Jaillon F, et al. High-penetration swept source Doppler optical coherence angiography by fully numerical phase stabilization. *Opt Express* 2012;20(3):2740–2760.
15. Nguyen QD, Brown DM, Marcus DM, et al. Ranibizumab for diabetic macular edema: results from 2 phase III randomized trials: RISE and RIDE. *Ophthalmology* 2012;119(4):789–801.
16. Yu L, Chen Z. Doppler variance imaging for three-dimensional retina and choroid angiography. *J Biomed Opt* 2010;15(1):016029.
17. Makita S, Hong Y, Yamanari M, Yatagai T, Yasuno Y. Optical coherence angiography. *Opt Express* 2006;14(17):7821–7840.
18. Szkulmowska A, Szkulmowski M, Szigal D, Kowalczyk A, Wojtkowski M. Three-dimensional quantitative imaging of retinal and choroidal blood flow velocity using joint spectral and time domain optical coherence tomography. *Opt Express* 2009;17(13):10584–10598.
19. An L, Wang RK. In vivo volumetric imaging of vascular perfusion within human retina and choroids with optical micro-angiography. *Opt Express* 2008;16(15):11438–11452.
20. Schwartz DM, Fingler J, Kim DY, et al. Phase-variance optical coherence tomography: a technique for noninvasive angiography. *Ophthalmology* 2014;121(1):180–187.
21. Mariampillai A, Leung MK, Jarvi M, et al. Optimized speckle variance OCT imaging of microvasculature. *Opt Lett* 2010;35(8):1257–1259.
22. Jia Y, Bailey ST, Wilson DJ, et al. Quantitative optical coherence tomography angiography of choroidal neovascularization in age-related macular degeneration. *Ophthalmology* 2014;121(7):1435–1444.
23. Hendargo HC, Estrada R, Chiu SJ, Tomasi C, Farsiu S, Izatt JA. Automated non-rigid registration and mosaicing for robust imaging of distinct retinal capillary beds using speckle variance optical coherence tomography. *Biomed Opt Express* 2013;4(6):803–821.
24. Newman DK. Surgical management of the late complications of proliferative diabetic retinopathy. *Eye (Lond)* 2010;24(3):441–449.
25. Imesch PD, Bindley CD, Wallow IH. Clinicopathologic correlation of intraretinal microvascular abnormalities. *Retina* 1997;17(4):321–329.
26. Kraus MF, Potsaid B, Mayer MA, et al. Motion correction in optical coherence tomography volumes on a per A-scan basis using orthogonal scan patterns. *Biomed Opt Express* 2012;3(6):1182–1199.
27. Klein T, Wieser W, Reznicek L, Neubauer A, Kampik A, Huber R. Multi-MHz retinal OCT. *Biomed Opt Express* 2013;4(10):1890–1908.

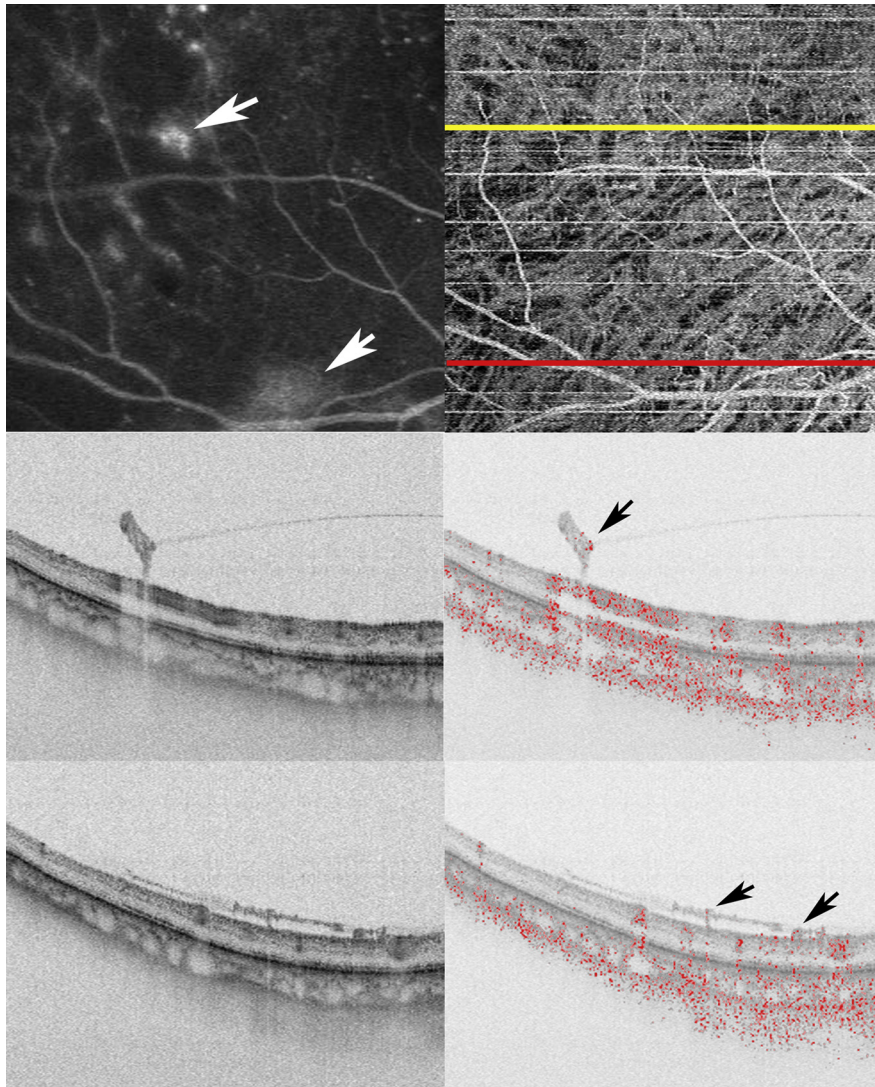


Biosketch

Masahiro Miura is an associate professor in Ophthalmology at Tokyo Medical University, Ibaraki Medical Center. He earned the MD degree from Nippon Medical School and PhD in Engineering from the University of Tsukuba. His specialties in research works are macular disease, polarization measurement, Doppler measurement, optical coherence tomography, and scanning laser ophthalmoscope.



SUPPLEMENTAL FIGURE 1. Doppler optical coherence tomography (OCT) image of the left eye of Subject 5 with tractional retinal detachment in proliferative diabetic retinopathy. The scanning area of the Doppler OCT image was 6.0×6.0 mm. Color fundus photography (Top row, left) and an en face projection image using standard OCT (Top row, middle) shows proliferative membranes in the disc. In the en face projection image using Doppler OCT (Top row, right), yellow and red lines indicate Doppler OCT B-scan images at the upper area (Second row) and the lower area (Third row), respectively. (Second row) Doppler OCT images at the upper area. A standard OCT image (left) shows tractional retinal detachment by vitreoretinal adhesion. A Doppler OCT composite image (right) shows the displacement of new vessels by vitreoretinal traction (black arrow). (Third row) Doppler OCT images of the lower area. A standard OCT image (left) shows tractional retinal detachment and a deformed loop formation. The Doppler OCT composite image (right) shows the presence of new vessels in the deformed loop formation (black arrow).



SUPPLEMENTAL FIGURE 2. Doppler optical coherence tomography (OCT) image of the right eye of Subject 6 with advanced neovascularization elsewhere in proliferative diabetic retinopathy. The scanning area of the Doppler OCT image was 6.0×6.0 mm. Fluorescein angiography (Top row, left) shows fluorescein leakage from the neovascularization (white arrows). Yellow and red lines in the en face projection image using Doppler OCT (Top row, right) specify the scanning line of the Doppler OCT B-scan images in the upper and lower areas, respectively (Second row and Third row). (Second row) Doppler OCT images at the upper area. A standard OCT image (left) shows the adhesion of proliferative tissue to the posterior hyaloid membrane. The Doppler OCT composite image (right) shows the presence of new vessels next to this adhesion (black arrow). (Third row) Doppler OCT images at the lower area. A standard OCT image (left) shows multiple adhesions to the proliferative tissue, and the Doppler OCT composite image (right) shows the presence of new vessels in these multiple adhesions (black arrows).